



September 10 - 12, 2007

Pilsen, Czech Republic

THE REVERSE RECONSTRUCTION RESULTS OBTAINED FROM THE NUMERICAL SIMULATION OF MR SIGNALS

ING. EVA KROUTILOVÁ, PHD.

ING. MICHAL HADINEC

ING. MILOSLAV STEINBAUER, PHD.

ING. MILOSLAV STEINBAUER, PHD.

DOC. ING. PAVE FIALA, PHD.

DOC. ING. KAREL BARTUŠEK, DRSC.

Abstract: The paper describes the magnetic resonance imaging method applicable mainly in MRI and MRS *in vivo* studies. We solved the effect of changes of magnetic fields in MR tomography. This article deals with the reverse reconstruction results obtained from the numerical simulation of MR signals by various techniques, which will be usable for the experimental results verification.

Key words: Numerical simulation, NMR

1 GEOMETRICAL MODEL

Fig. 1 describes the sample geometry for the numerical modeling. On both sides, the sample is surrounded by the referential medium. During the real experiment, the reference is represented by water, which is ideal for obtaining the MR signal.

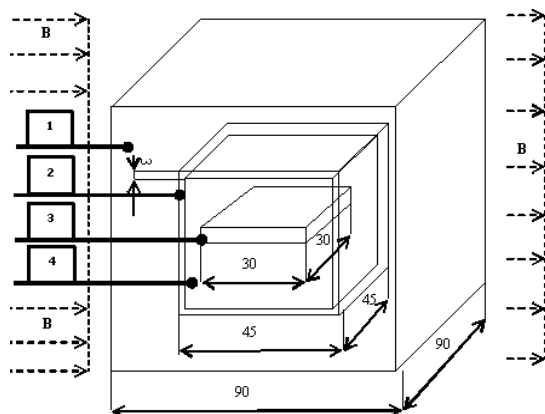


Fig. 1 The sample geometry for numerical modeling

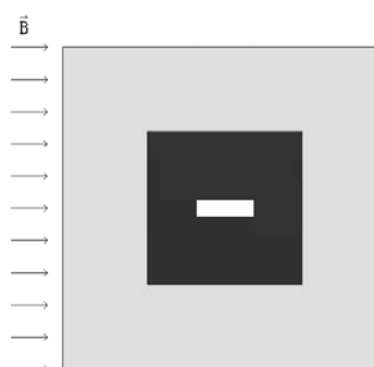


Fig. 2 The geometrical model in the system Ansys

As shown in fig. 1, in the model there are defined four volumes with different susceptibilities. The materials are defined by their permeabilities: material No. 1 – the medium outside the cube (air), $\chi = 0$, material No. 2 – the cube walls (sodium glass), $\chi = -11,67 \cdot 10^{-6}$, material No. 3 is the sample material (sodium glass), $\chi = -11,67 \cdot 10^{-6}$, quartz glass, $\chi = -8,79 \cdot 10^{-6}$, the simax glass (commercial

name), $\chi = -8,82 \cdot 10^{-6}$, material No.4 is the medium inside the cube (water with nickel sulfate solution NiSO₄, $\chi = -12,44 \cdot 10^{-6}$). The permeability rate was set with the help of the relation $\mu=1+\chi$. For the sample geometry according to fig. 1, the geometrical model was built in the system. In the model there was applied the discretization mesh with 133584 nodes and 126450 elements, type Solid96 (Ansys). The boundary conditions (1) were selected for the induction value of the static elementary field to be $B_0 = 4,7000$ T in the direction of the z coordinate (the cube axis) – corresponds with the real experiment carried out using the MR tomograph at the Institute of Scientific Instruments, ASCR Brno.

2 NUMERICAL ANALYSIS

The numerical modelling was realized using the finite element method together with the Ansys system. As the boundary condition, there was set the scalar magnetic potential ϕ_m by solving Laplace's equation

$$\Delta \phi_m = \text{div } \mu(-\text{grad } \phi_m) = 0 \quad (1)$$

together with the Dirichlet boundary condition

$$\phi_m = \text{konst.} \quad \text{on the areas } \Gamma_1 \text{ and } \Gamma_2$$

and the Neumann boundary condition

$$\mathbf{u}_n \cdot \text{grad } \phi_m = 0 \quad \text{on the areas } \Gamma_3 \text{ and } \Gamma_4. \quad (3)$$

The continuity of tangential elements of the magnetic field intensity on the interface of the sample region is formulated by the expression

$$\mathbf{u}_n \times \text{grad } \phi_m = 0 \quad (4)$$

The description of the quasi-stationary model MKP is based on the reduced Maxwell's equations

$$\text{rot } \mathbf{H} = \mathbf{J} \quad (5)$$

$$\text{div } \mathbf{B} = 0 \quad (6)$$

where \mathbf{H} is the magnetic field intensity vector, \mathbf{B} is the magnetic field induction vector, \mathbf{J} is the current density vector. For the case of the static magnetic irrotational field, the equation (5) is reduced to the expression (7).

$$\text{rot } \mathbf{H} = 0 \quad (7)$$

Material relations are represented by the equation

$$\mathbf{B} = \mu_0 \mu_r \mathbf{H} \quad (8)$$

where μ_0 is the permeability of vacuum, $\mu_r(B)$ is the relative permeability of ferromagnetic material. The closed area Ω , which will be applied for solving the equations (6) and (7), is divided into the region of the sample Ω_1 and the region of the medium Ω_2 . For these, there holds $\Omega = \Omega_1 \cup \Omega_2$. For the magnetic field intensity H in area Ω there holds the relation (7). The magnetic field distribution from the winding is expressed with the help of the Biot-Savart law, which is formulated as

$$\mathbf{T} = \frac{1}{4\pi} \int_{\Omega} \frac{\mathbf{J} \times \mathbf{R}}{|\mathbf{R}|^3} d\Omega \quad (9)$$

where \mathbf{R} is the distance between a point in which the magnetic field intensity \mathbf{T} is looked for and a point where

the current density \mathbf{J} is assumed. The magnetic field intensity \mathbf{H} in the area can be expressed as

$$\mathbf{H} = \mathbf{T} - \text{grad } \phi_m \quad (10)$$

where \mathbf{T} is the preceding or estimated magnetic field intensity, ϕ_m is the magnetic scalar potential. The boundary conditions are written as

$$\mathbf{u}_n \cdot \mu(\mathbf{T} - \text{grad } \phi_m) = 0 \quad (11)$$

on the areas Γ_3 and Γ_4 .

where \mathbf{u}_n is the normal vector, Γ_{Fe-0} is the interface between the areas Ω_{Fe} and $\Omega_0 \cup \Omega_w$. The area Ω_0 is the region of air in the model, the area Ω_w is the region with the winding. The continuity of tangential elements of the magnetic field intensity on the interface of the area with ferromagnetic material is expressed

$$\mathbf{u}_n \times (\mathbf{T} - \text{grad } \phi_m) = 0 \quad (12)$$

By applying the relation (10) in the relation (11) we get the expression

$$\text{div } \mu_0 \mu_r \mathbf{T} - \text{div } \mu_0 \mu_r \text{grad } \phi_m = 0 \quad (13)$$

The equation can be discretized (13) by means of approximating the scalar magnetic potential

$$\phi_m = \sum_{j=1}^{NN} \varphi_j W_j(x, y, z) \quad (2)$$

$$(14)$$

$$\text{pro } \forall (x, y, z) \in \Omega$$

where φ_j is the value of the scalar magnetic potential in the j-th node, W_j the approximation function, NN the number of nodes of the discretization mesh. By applying the approximation (14) in the relation (13) and minimizing the residues according to the Galerkin method, we get the semidiscrete solution

$$\sum_{j=1}^{NN} \varphi_j \int_{\Omega} \mu \text{grad } W_i \cdot \text{grad } W_j d\Omega = 0 \quad (15)$$

$$i = 1, \dots, NN$$

The system of equations (15) can be written briefly as

$$\begin{bmatrix} k_{ij} \end{bmatrix} \cdot \begin{bmatrix} \varphi_i \end{bmatrix}^T = 0 \quad i, j \in \{1, \dots, NN\} \quad (16)$$

The system (16) can be divided into

$$\mathbf{K} \begin{bmatrix} \mathbf{U}_I \\ \mathbf{U}_D \end{bmatrix} = \begin{bmatrix} \mathbf{0} \\ \mathbf{0} \end{bmatrix}, \quad (17)$$

where $\mathbf{U}_I = [\varphi_1, \dots, \varphi_{NI}]^T$ is the vector of unknown internal nodes of the area Ω including the points on the areas Γ_3 and Γ_4 . $\mathbf{U}_D = [\varphi_1, \dots, \varphi_{ND}]^T$ is the vector of known potentials on the areas Γ_1 and Γ_2 (the Dirichlet boundary conditions). NI in the index marks the number of internal nodes of the discretization mesh, ND is the number of the mesh boundary nodes. Then, the system can be written further in 4 submatrixes

The system of equations (16) can be solved with the help of standard algorithms. The scalar magnetic potential value is then used for evaluating the magnetic field intensity according to (10).

3 NUMERICAL MODEL

The numerical modelling results are represented in fig.2 and fig.7. The numerical modelling results were then used for the representation of the module of

magnetic induction \mathbf{B} along the defined path. For the model meshing, the element size selected as optimum was $0,5 \cdot 10^{-3} \text{m}$. The boundary conditions $\pm\varphi/2$ were set to the model edges, to the external left and right boundaries of the air medium, as represented in fig.1. The excitation value $\pm\varphi/2$ was set using again the relation (21). This is derived for the assumption that, in the entire area, there are no exciting currents, therefore there holds for the *rot* $\mathbf{H} = 0$ and the field is irrotational.

Consequently, for the scalar magnetic potential φ_m holds

$$H = -\text{grad}\varphi_m \quad (18)$$

The potential of the exciting static field with intensity \mathbf{H}_0 is by applying (18)

$$\varphi_m = \int \vec{H}_0 \cdot \vec{u}_z dz = H_0 \cdot z \quad (19)$$

where

$$H_0 = \frac{B}{\mu_0 \cdot \mu_r} \quad (20)$$

Then

$$\pm \frac{\varphi}{2} = \frac{B \cdot z}{2\mu_0} = \frac{4,7000 \text{ T} \cdot 90 \text{ mm}}{2\mu_0} \quad (21)$$

where z is the total length of the model edge.

4 EXPERIMENTAL VERIFICATION

The experimental measuring was realized using the MR tomograph at the Institute of Scientific Instruments, ASCR Brno. The tomograph elementary field $B_0 = 4,7000 \text{ T}$ is generated by the superconductive solenoidal horizontal magnet produced by the Magnex Scientific company. The corresponding resonance frequency for the ^1H cores is 200 MHz.

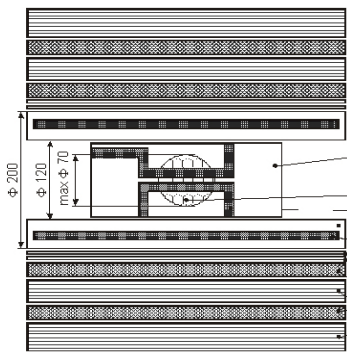


Fig. 3 Elementary configuration of the MR magnet for the 200MHz tomograph, ISI ASCR

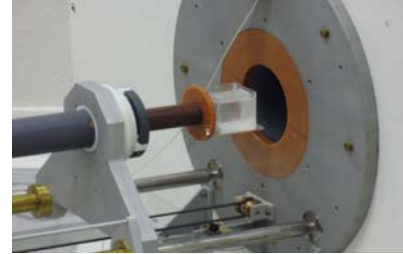


Fig. 4 The measured preparation. The preparation seating in the tomograph

5 THE COMPARISON OF RESULTS: NUMERICAL MODELLING AND MEASURING

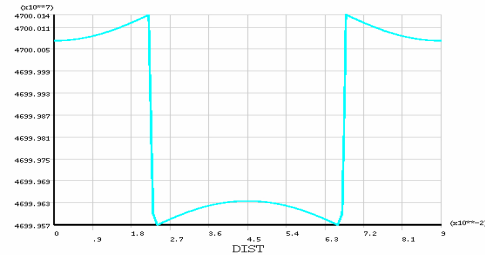


Fig. 5 The magnetic induction B pattern, numerical model, without the sample

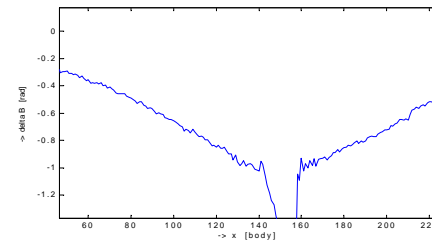


Fig. 6 The measured pattern of magnetic induction B , through the medium, without the Sample

6 CONCLUSION

The numerical modelling and analysis of the task have verified the experimental results and, owing to the modifiability of the numerical model, we have managed to advance further in the experimental qualitative NMR image processing realized at the ISI ASCR

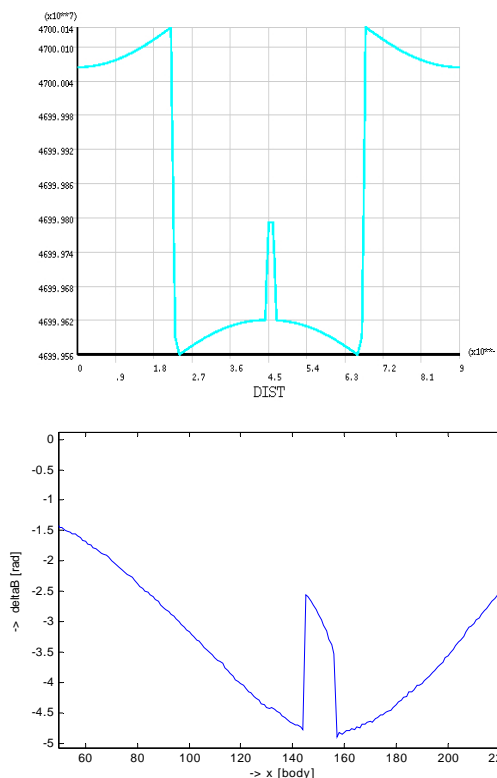


Fig. 7 The magnetic induction B pattern, numerical model, quartz glass, $\Delta B = 17 \mu T$

ACKNOWLEDGEMENT

The research described in the paper was financially supported by research plans GAAV B208130603, MSM 0021630516 and GA102/07/0389.

REFERENCES

[1] Fiala, P., Kroutilová, E., Bachorec, T. Modelování elektromagnetických polí, počítačová cvičení. vyd. Brno: VUT v Brně, FEKT, Údolní 53, 602 00, Brno, 2005. s. 1 - 69 .

[2] Steinbauer, M. Měření magnetické susceptivity technikami tomografie magnetické rezonance. vyd. Brno: VUT v Brně, FEKT, Údolní 53, 602 00, Brno, 2006.

Assoc. Prof. Pavel Fiala, Ph.D., Ing. Eva Kroutilova, Ph.D., Ing. Miloslav Steinbauer, Ph.D., Ing. Michal Hadinec
Brno University of Technology, Faculty of Electrical Engineering and Communication, Department of Theoretical and Experimental Electrical Engineering, Kolejni 2906/4, 612 00 Brno, Czech Republic
<http://www.utee.feec.vutbr.cz/EN/index.htm>, tel: +420 541 149 510, email: fialap@feec.vutbr.cz, krutila@feec.vutbr.cz, steinbau@feec.vutbr.cz, xhadin00@stud.feec.vutbr.cz

Assoc. Prof. Ing. Karel Bartusek, CSc.
Academy of Sciences of the Czech Republic,
Institute of Scientific Instruments, Kralovopolska 147, 612 64 Brno, Czech Republic